ELSEVIER

Nuclear Instruments and Methods in Physics Research B 181 (2001) 231–237

NIM B
Beam Interactions with Materials & Atoms

www.elsevier.com/locate/nimb

Channeling contrast microscopy on lateral epitaxial overgrown GaN

E.J. Teo [a,*], T. Osipowicz [a], A.A. Bettiol [a], F. Watt [a], M.S. Hao [b], S.J. Chua [b]

[a] *Department of Physics, Research Centre for Nuclear Microscopy (RCNM), National University of Singapore, Lower Kent Ridge Road, Singapore 119260, Singapore*

[b] *Institute of Materials Research and Engineering (IMRE), 3 Research Link, Singapore 117602, Singapore*

Abstract

High resolution (<1 μm) channeling contrast microscopy (CCM) is employed to map variations of crystallographic orientation across micron-sized regions of lateral epitaxial overgrown (LEO) GaN thin film structures. The sample consists of 6 μm thick GaN stripes, aligned along the $[1\bar{1}00]_{GaN}$ direction, grown by LEO from 3 μm wide Si_3N_4 windows spaced 13 μm apart. Axial CCM using 2 MeV He^+ is employed to investigate the crystalline structure of the LEO GaN layer. A low χ_{min} of ~2.8% and a critical angle $\psi_{1/2}$ of ~0.85° is found, comparable with data obtained from broad beam channeling [J. Portmann, C. Huag, R. Benn, T. Frey, B. Schottker, D.J. As, Nucl. Instr. and Meth. B 155 (1999) 489]. 5 μm wide bands of high and low yield at a periodicity of 13 μm are observed in the CCM maps. This contrast is due to the opposing tilts of the [0 0 0 1] axis in the overgrown regions (the so-called wings) on either side of the window regions. From angular scan curves this tilt is found to be ±0.45° in the direction perpendicular to the GaN stripes and no measurable wing tilt is found along the stripe direction. © 2001 Elsevier Science B.V. All rights reserved.

PACS: 7.78.+S; 61.85.+P; 82.80.YC

---

1. Introduction

Lateral epitaxial overgrowth (LEO) has been shown to significantly reduce the density of extended defects in GaN films grown by metal organic chemical vapor deposition (MOCVD) and hybrid vapor phase epitaxy (HVPE) on sapphire and SiC substrates [1,2]. This reduction in threading dislocation density (TDD) has recently led to benefits in device performance such as longer lifetime cw blue laser [3], low reverse bias leakage current light emitting diodes [4] and p–n junctions [5], and low gate leakage current $Al_xGa_{1-x}N$/GaN field-effect transistors.

Despite these advantages of device performance on LEO GaN compared to conventional GaN films, difficulties remain in controlling the structural quality of the overgrown material, such as the tilting of crystal planes in overgrown regions (wings) with respect to those of the window region [6,8,9]. Although the mechanism behind the wing

---

[*] Corresponding author.
E-mail address: scip8064@nus.edu.sg (E.J. Teo).

PII: S0168-583X(01)00460-8

tilt is not fully understood, it has been empirically correlated with the ratio of the overgrowth width with its height [6,7].

X-ray diffraction (XRD) has been used to measure wing tilt with the scattering plane perpendicular to the stripe direction [6,8,9]. However, this technique is unable to provide laterally resolved information of the crystallographic tilts across the GaN stripes. In this work, we report the use of channeling contrast microscopy (CCM) to image crystallographic tilting in micron-sized overgrown regions of LEO GaN. By performing angular scans perpendicular to the GaN stripes, it is possible to determine the wing tilt relative to the window region. The CCM maps reveal bands of high and low contrast, separated by 13 μm which correspond to overgrown regions of opposite wing tilts. Line projections along the stripe direction of the CCM maps are plotted to show the lateral changes in the channeled yield for a given beam incidence angle.

2. Experimental

Lateral overgrown GaN stripes, patterned by the underlying Si_3N_4 mask, were deposited on GaN buffer layer/[0 0 0 1] Al_2O_3 substrate. Initially, a 2 μm thick GaN seed layer was grown by MOCVD (40 min) on a *c*-plane sapphire substrate. A 100 nm SiN mask layer was deposited on GaN by plasma-enhanced chemical vapor deposition (PECVD) and then patterned into $[1\bar{1}00]_{GaN}$ oriented stripes which define a 3 μm opening (window) at a periodicity of 13 μm. The lateral overgrowth GaN layer was achieved at a pressure of 100 Torr, with trimethlygallium (TMG) and NH_3 at a flow rate of 123 μmol/min and 10 000 sccm, respectively, in combination with 6000 sccm of H_2 diluent. After 3.5 h of LEO growth on the mask, GaN stripes of 6 μm thickness propagated vertically through the window, with a width of 12.8 μm over the mask so that the stripes are close to coalescence (see Fig. 1).

Characterization of LEO GaN was carried out using the new 3.5 MeV singletron accelerator [10] at the National University of Singapore. Initially, 2 MeV He^+ broad beam channeling was used to find the [0 0 0 1] axial position and subsequently the beam was focused down to 1 μm spot size. For microbeam channeling experiments, a beam current of typically 50–100 pA was used. The collimators were set so that the divergence of beam was less than 0.2°. This condition provides reasonable channeling as the beam divergence is significantly less than the critical half angle of 0.8° along the major axis of GaN. Previous measurements of wing tilts on similar LEO GaN samples were done

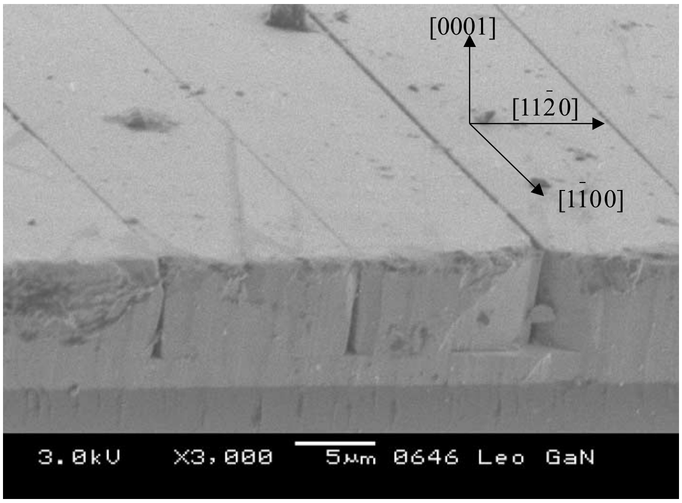

Fig. 1. Cross-section SEM picture of LEO GaN stripes.

using XRD by measuring an ω rocking curve about the GaN 0002 peak, with the scattering plane perpendicular to the stripes [6,8,9]. In order to obtain comparable data, the angular scan was performed through the axial direction of [0 0 0 1] across the GaN stripes, along the $[1\,1\,\bar{2}\,0]$ direction. The sample was mounted in such a way that the GaN stripes were aligned with the y-axis, and then rotated around the y-axis. Channeling RBS spectra were recorded with 300 mm^2 PIPS detector of 19 keV energy resolution at a scattering angle of 145°. A large solid angle of 222 msr was used because of the limited beam current available. The target was mounted on a eucentric goniometer with a 24 mm translational range for both the x and y direction that allows rotations around the x- and y-axis with a resolution of 0.025°. The beam was scanned over an area of 50×50 μm^2. The average collection time was about 30 min.

The sample was also characterized by scanning electron microscopy (SEM) at 3 kV.

3. Results

Fig. 1 shows a cross-sectional SEM micrograph of the LEO GaN just before coalescence. The GaN stripes have a thickness of 6 μm, with a width of 12.8 μm and a periodicity of 13 μm. These gaps would not be visible in the CCM maps due to the limited beam resolution.

The laterally resolved channeling data has been extracted from the RBS spectra in surface-near regions (<1 μm) of the GaN layer. Fig. 2 shows the random and channeled spectra of the LEO GaN. A $\chi_{\min}$ of 2.8% is obtained in the $[0\,0\,0\,1]_{\mathrm{GaN}}$ direction using scanning microbeam channeling, indicating excellent crystal quality. The high resolution CCM map shown in Fig. 3 reveals 5 μm wide regions of alternating high yield at a periodicity of 13 μm. Because of the difficulty of positioning the sample precisely at the eucentric point of the goniometer, and possible mechanical backlash, the goniometer produces lateral shifts of the sample position (typically 2 μm per 0.2°). Therefore a defect present in the sample was used to align the CCM maps for different tilt angles as seen in Figs. 4(b)–(d). It can be seen from Fig. 4(b) that certain bands (band A in Fig. 4(a)) appearing dark (large channeling yield) at 0.143°, get brighter (less channeling yield) as the sample is tilted towards 0.143°. Similarly, bands B defined in Fig. 4(a) appearing bright at −0.143° become darker when tilted towards the 0.143°. This is demonstrated by the projections of the maps to the x-axis shown in

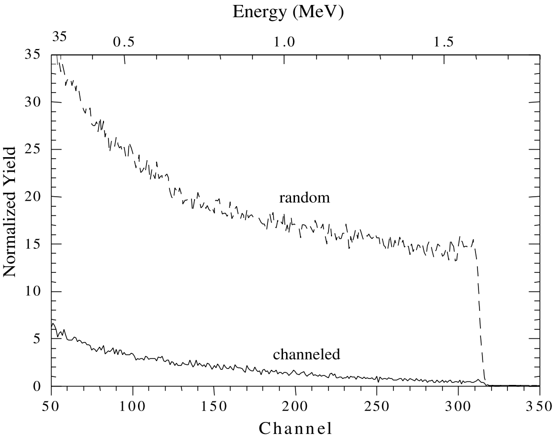

Fig. 2. RBS spectra of random and [0 0 0 1] channeled GaN.

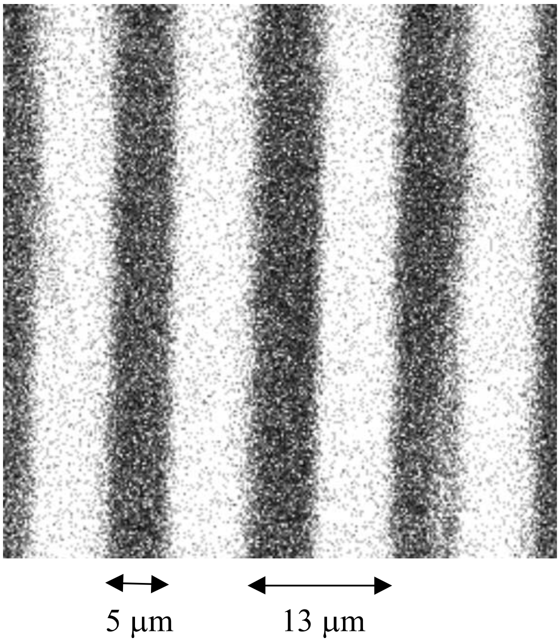

Fig. 3. CCM map of LEO GaN.

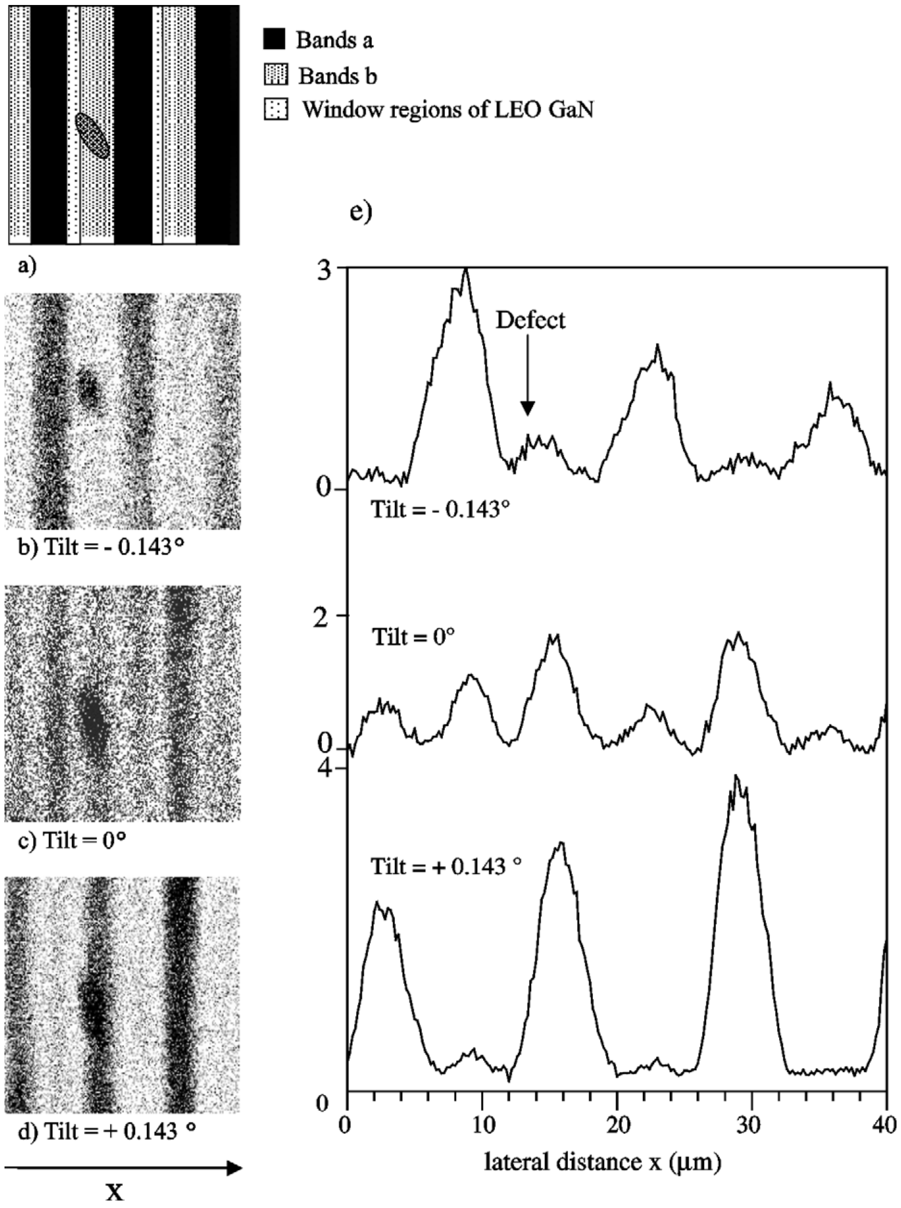

Fig. 4. (a) Schematic diagram of bands A and B in CCM map. CCM maps showing the line patterns of opposite contrast at tilt angles of (b) −0.143°, (c) 0°, (d) +0.143° with the help of defect. (e) Projections of channeled yield to x-axis for tilt angles of −0.143°, 0°, 0.143°.

Fig. 4(e). Clearly, the yield of band A observed at negative tilt angles decreases significantly as the sample is tilted towards positive values. The yield from band B, on the other hand, increases from negative tilt angles to a maximum at positive tilt angles. At the [0 0 0 1] position, the number of peaks observed is doubled, but at a smaller magnitude. From these observations, it can be concluded that the overgrown regions (bands A and B), with a width of 5 μm at a periodicity of 13 μm,

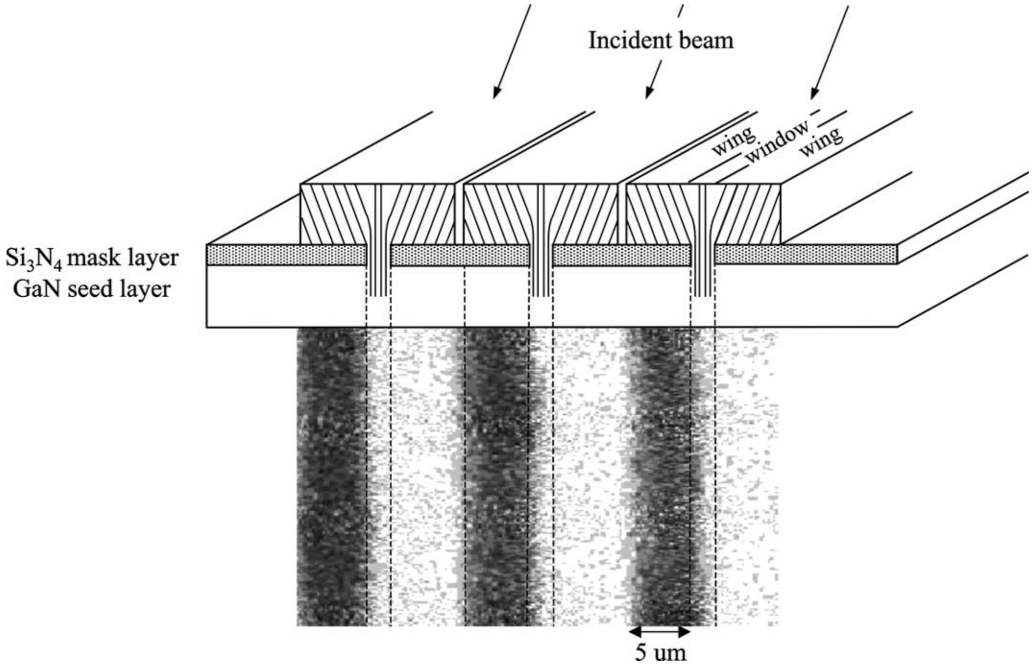

Fig. 5. Origins of the contrast patterns observed in the CCM maps.

have opposing plane tilts. Fig. 5 illustrates the situation. In the axial direction, slight dechanneling is observed from both sides of the overgrown region, with low channeling yields from the window region. As the tilt angle moves to 0.143°, the CCM maps show high yields from band B and low yields from band A. Similarly, band A shows high yields when the tilt angle is set to −0.143°.

All data are collected in list-mode, making it possible to extract separate rocking curves from band A to B (as shown in Fig. 4(a)). Fig. 6 shows these angular scans, half angles $\psi_{1/2}$ of ~0.85° are obtained for bands A and B. The angular scan curves are also displaced by ±0.45° from the [0 0 0 1] GaN seed layer direction. No wing tilt is observed along the stripe direction when the sample is rotated about the x direction.

For larger tilting angles, beyond ±0.75°, a broadening of the bands can be observed in the CCM maps, so that regions A and B can no longer be identified. This is demonstrated in Fig. 7, showing the line projection of the CCM yield across a GaN stripe for different tilt angles. There

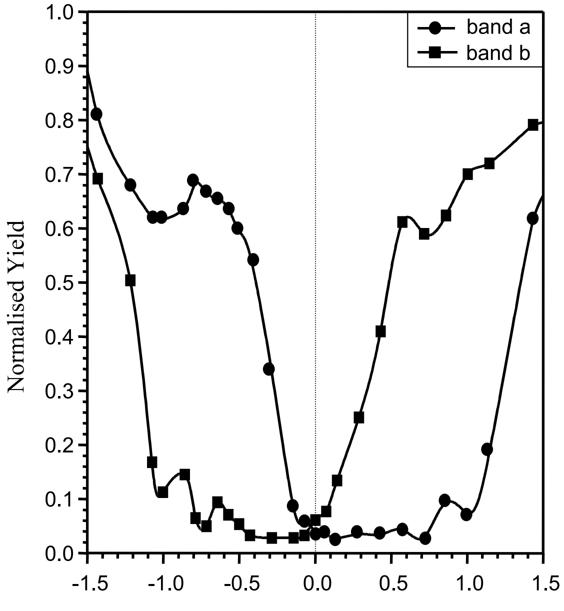

Fig. 6. Displacement of angular scan curves by ±0.45° in regions A and B.

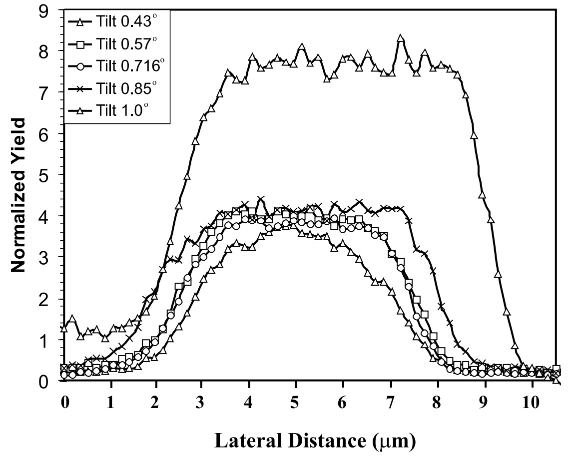

Fig. 7. Widening of the bands for tilt angles from 0.43° to 1.0°.

is no observable increase in the width of the bands when the tilt angle is increased from 0.57° to 0.716°. However, the width broadens significantly from 6.3 μm at 0.85° to 7 μm at 1.0°. This broadening effect can be explained by the dechanneling that occurs in the region of opposite orientation (see Fig. 6). The shoulders observed on each angular scan curve in Fig. 6 might be due to the emerging yield from each of the opposite sides, although this point is still under investigation.

The amount of damage produced by the He ion beam is estimated by a comparison of the spectra produced by the first and last 15% of the charge in a long CCM run (see Fig. 8). These channeled spectra, taken at a average doses of 4.7×10^{15} and 5.3×10^{16} He^+/cm^2, are very similar, confirming that negligible damage accumulates on the sample for doses of 5.3×10^{16} He^+/cm^2 (8.5 mC/cm^2) which are typically used for each run. It was estimated by Ingarfield et al. [11] that significant lattice damage happens when He^+ fluence exceeds 6.2×10^{17} He^+/cm^2.

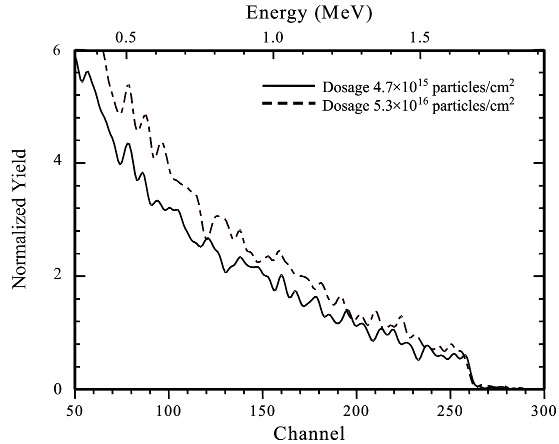

Fig. 8. Comparison of spectra taken at 4.7×10^{15} and 5.3×10^{16} He^+/cm^2.

4. Conclusion

High resolution CCM has been successfully employed to investigate the tilting planes of micron-sized overgrown regions of LEO GaN stripes. CCM measurements show 5 μm wide overgrown regions with crystallographic tilt of ±0.45° from the [0 0 0 1] axis of the seed layer at a periodicity of 13 μm. This wing tilt is found to be perpendicular to the $[1\bar{1}00]_{\mathrm{GaN}}$ stripe direction, with no observable tilt in the stripe direction. CCM is shown to be a powerful analytical tool, because no other method allows the imaging of lattice tilts in micron-sized regions without tedious sample preparation procedures.

Acknowledgements

The authors would like to thank Micky Leong for the SEM measurement.

References

[1] H. Marchand, X.H. Wu, J.P. Ibbetson, P. Fini, P. Kozodoy, S. Keller, J.S. Speck, S.P. DenBaars, U.K. Mishra, Appl. Phys. Lett. 73 (1998) 747.
[2] K.J. Linthicum, T. Gehrke, D.B. Thomson, E.P. Carlson, P. Rajagopal, T.P. Smith, A.D. Batchelor, R.F. Davis, Appl. Phys. Lett. 75 (1999) 196.
[3] S. Nakamura, M. Senoh, S.I. Nagahama, N. Iwasa, T. Yamada, T. Matsushita, H. Kiyoku, Y. Sugimoto, T. Kozaki, H. Umemoto, M. Sano, K. Chocho, J. Cryst. Growth 189/190 (1998) 820.
[4] C. Sasaoka, H. Sunakawa, A. Kimura, M. Nido, A. Usui, A. Sakai, J. Cryst. Growth 189/190 (1998) 61.

[5] P. Kozodoy, J.P. Ibbetson, H. Marchand, P. Fini, S. Keller, J.S. Speck, S.P. DenBaars, U.K. Mishra, Appl. Phys. Lett. 73 (1998) 975.
[6] P. Fini, J.P. Ibbetson, H. Marchand, L. Zhao, S.P. DenBaars, J.S. Speck, J. Cryst. Growth 209 (2000) 581.
[7] O.-H. Nam, M.D. Bremser, T.S. Zheleva, R.F. Davis, Appl. Phys. Lett. 71 (18) (2000) 2638.
[8] P. Fini, L. Zhao, B. Noran, M. Hansen, H. Marchand, J.P. Ibbetson, S.P. DenBaars, U.K. Mishra, J.S. Speck, Appl. Phys. Lett. 75 (1999) 1706.
[9] P. Fini, A. Munkholm, C. Thompson, G.B. Stephenson, J.A. Eastman, M.V. Ramana Murty, O. Auciello, L. Zhao, S.P. DenBaars, J.S. Speck, Appl. Phys. Lett. 76 (26) (2000) 3893.
[10] D.J.W. Mous, R.G. Haitsma, T. Butz, R.H. Flagmeyer, D. Lehmann, J. Vogt, Nucl. Instr. and Meth. B 130 (1997) 31.
[11] S.A. Ingarfield, C.D. McKenzie, K.T. Short, J.S. Williams, Nucl. Instr. and Meth. 191 (1981) 521.